Environmental Toxicology and Pharmacology 107 (2024) 104417

Contents lists available at ScienceDirect

Environmental Toxicology and Pharmacology

journal homepage: www.elsevier.com/locate/etap

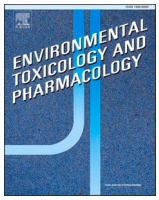

AuNPs with Cynara scolymus leaf extracts rescue arsenic-induced neurobehavioral deficits and hippocampal tissue toxicity in Balb/c mice through D1R and D2R activation

Betul Cicek [a], Ahmet Hacimuftuoglu [b], Yesim Yeni [c], Mehmet Kuzucu [d], Sidika Genc [e], Ahmet Cetin [d], Emre Yavuz [f], Betul Danısman [g], Akin Levent [h], Kemal Volkan Ozdokur [i], Mecit Kantarcı [j], Anca Oana Docea [k,*], Vasileios Siokas [l], Konstantinos Tsarouhas [m], Michael D. Coleman [n], Aristidis Tsatsakis [o,*], Ali Taghizadehghalehjoughi [e]

[a] Department of Physiology, Faculty of Medicine, Erzincan Binali Yildirim University, Erzincan 24100, Turkey
[b] Department of Medical Pharmacology, Faculty of Medicine, Ataturk University, Erzurum 25240, Turkey
[c] Department of Medical Pharmacology, Faculty of Medicine, Malatya Turgut Ozal University, Malatya 44210, Turkey
[d] Department of Biology, Faculty of Arts and Sciences, Erzincan Binali Yildirim University, Erzincan 24100, Turkey
[e] Bilecik Şeyh Edebali University, Faculty of Medicine, Department of Medical Pharmacology, Bilecik 11230, Turkey
[f] Department of Medical Services and Technicians, Çayirli Vocational School, Erzincan Binali Yildirim University, Erzincan, Turkey
[g] Department of Biophysics, Faculty of Medicine, Ataturk University, Erzurum 25240, Turkey
[h] Department of Radiology, Faculty of Medicine, Erzincan Binali Yildirim University, Erzincan 24100, Turkey
[i] Sciences Application and Research Center, Erzincan Binali Yildirim University, Erzincan 24100, Turkey
[j] Department of Radiology, Faculty of Medicine, Ataturk University, Erzurum 25240, Turkey
[k] Department of Toxicology, University of Medicine and Pharmacy of Craiova, Craiova, Romania
[l] Department of Neurology, University Hospital of Larissa, Faculty of Medicine, School of Health Sciences, University of Thessaly, Larissa 41100, Greece
[m] Department of Cardiology, University Hospital of Larissa, Larissa 41100, Greece
[n] College of Health and Life Sciences, Aston University, Birmingham B4 7ET, UK
[o] Department of Forensic Sciences and Toxicology, Faculty of Medicine, University of Crete, Heraklion 71003, Greece

ARTICLE INFO

Keywords:
AuNPs
Arsenic
Cynara scolymus
Neurotoxicity
D1R
D2R

ABSTRACT

The present study was designed to evaluate whether AuNPs (gold nanoparticles) synthesized with the *Cynara scolymus* (CS) leaf exert protective and/or alleviative effects on arsenic (As)-induced hippocampal neurotoxicity in mice. Neurotoxicity in mice was developed by orally treating 10 mg/kg/day sodium arsenite ($NaAsO_2$) for 21 days. 10 μg/g AuNPs, 1.6 g/kg CS, and 10 μg/g CS-AuNPs were administered orally simultaneously with 10 mg/kg As. CS and CS-AuNPs treatments showed down-regulation of TNF-α and IL-1β levels. CS and CS-AuNPs also ameliorated apoptosis and reduced the alterations in the expression levels of D1 and D2 dopamine receptors induced by As. Simultaneous treatment with CS and CS-AuNPs improved As-induced learning, memory deficits, and motor coordination in mice assessed by water maze and locomotor tests, respectively. The results of this study provide evidence that CS-AuNPs demonstrated neuroprotective roles with antioxidant, anti-inflammatory, and anti-apoptotic effects, as well as improving D1 and D2 signaling, and eventually reversed neurobehavioral impairments.

1. Introduction

According to its known or suspected toxicity, arsenic is the top toxin that poses a significant threat to human health. (Hughes et al., 2011; Wallace et al., 2020). Approximately 230–300 million individuals worldwide consume water contaminated with levels of arsenic above the

* Corresponding authors.
E-mail addresses: ahmeth@atauni.edu.tr (A. Hacimuftuoglu), yesimyeni.75@outlook.com.tr (Y. Yeni), mkuzucu@erzincan.edu.tr (M. Kuzucu), emre.yavuz@erzincan.edu.tr (E. Yavuz), betul.danisman@atauni.edu.tr (B. Danısman), alevent@erzincan.edu.tr (A. Levent), vozdokur@erzincan.edu.tr (K.V. Ozdokur), ancadocea@gmail.com (A.O. Docea), m.d.coleman@aston.ac.uk (M.D. Coleman), tsatsaka@uoc.gr (A. Tsatsakis), ali.tgzd@bilecik.edu.tr (A. Taghizadehghalehjoughi).

https://doi.org/10.1016/j.etap.2024.104417

Available online 15 March 2024

allowable limit (10 ppb) set by the World Health Organization (Shaji et al., 2021). Arsenic, which accumulates in several parts of the brain bypassing the blood-brain barrier, can deregulate several neuro-cellular signaling pathways and functions (Medda et al., 2020; Pandey et al., 2022; Rodríguez-Barranco et al., 2016; Vucinic et al., 2017).

The hypothalamic-pituitary-adrenocortical (HPA) axis and lymphoid organs (thymus, spleen, and bone marrow) are known to be particularly sensitive to chemicals and metals (Karaulov et al., 2022). The hippocampus, located in the temporal lobe, is crucial in working memory, and hippocampal neuronal atrophy is a principal reason for cognitive impairment (Lin et al., 2016; O'Callaghan et al., 2019). Dopamine (DA) is a well-known neurotransmitter of hippocampal synaptic plasticity and executes the modulation of learning and memory (Speranza et al., 2021). The D1 receptor (D1R) is believed to play a more significant role in synaptic plasticity, learning, and memory, although different dopamine receptor subtypes are involved in various aspects of learning and memory (Takeuchi et al., 2016). It has been postulated that D1R inactivation or pharmacological blockade in the hippocampus disturbs associative, spatial, and episodic-like memory (Takeuchi et al., 2016). Also, impaired D1R activation changes early long-term (LTP) potentiation and late LTP and reduces their progression by impairing the transition from one to the other (Granado et al., 2008). Although the exact role of the dopamine D2 receptor (D2R) on memory-related brain plasticity development is less clear, it is apparent that D2R performs memory consolidation and associative acquisition (Espadas et al., 2021). Evidence suggests that arsenic can drastically alter DA levels and dopamine receptors such as D1R and D2 in different brain regions, thereby influencing cognitive and behavioral abnormalities (Kim et al., 2014; Mehta et al., 2021).

Gold nanoparticles (AuNPs) may be applied in several domains, one of the most significant being the biomedical field. Additionally, due to their expansive surface and versatility in the types of therapeutic agents that can be applied to them, AuNPs have been reported to act successfully as drug delivery systems (Cabuzu et al., 2015; de Bem Silveira et al., 2021; Ribarič 2021).

Studies have reported that medicinal plant-mediated AuNPs have a protective effect in neurodegenerative diseases (Kumar and Yadav, 2009; Subakanman et al., 2015): this potential may be related to the natural source, plant-derived flavonoids and the unique particularities offered by the AuNPs. The utilization of AuNPs synthesized with herbal extracts offers flavonoid treatment the benefit of a protracted effect on the target organ in comparison with classical herbal extract preparations, thus potentiating their impact (Kumar and Yadav, 2009; Subakanman et al., 2015; Xue et al., 2019). The artichoke species *Cynara scolymus* (CS) is recognized as a medicinal plant applied in herbal medicine from ancient times (Ibrahim et al., 2022). Its leaf contains numerous phytoconstituents including phenolic, flavonoid, and tannins, and has potent different pharmacological properties like anti-inflammatory and antioxidant activities (Cicek et al., 2022; Ibrahim et al., 2022). Although classical CS preparations are thought to be potent and safe compounds for multiple medical applications (Cicek et al., 2022; Ibrahim et al., 2022) some undesirable pharmacokinetic characteristics such as reduced bioavailability of orally administered CS, rapid systemic elimination, and fast metabolism by the liver limit its therapeutic effectiveness (Xue et al., 2019). To overcome these problems, we think that CS formulation with AuNPs may improve its bioavailability and efficiency. Therefore, in this report, the effects of AuNPs utilizing the aqueous extract of *Cynara scolymus* leaf against arsenic-induced hippocampal toxicity are presented with the use of behavioral tests and biochemical analysis. Furthermore, mechanistic insight regarding the molecular mechanisms related to alterations in D1 and D2 signaling in the hippocampus is shown.

2. Materials and methods

2.1. Chemicals and reagents

Since every reagent was of analytical grade, no additional purification was necessary. Potassium tetrachloroaurate (III) ($KAuCl_4$) was provided by Sigma Aldrich (St. Louis, MO, USA). Ascorbic acid ($C_6H_8O_6$) was purchased from Merck Company (Germany). Ultra-pure water with 18.2 MΩ cm resistivity was utilized in all experiments. Sodium arsenite ($NaAsO_2$) obtained from Sigma Aldrich (St. Louis, MO, USA). All the ELISA kits were provided by Elabscience (Texas, USA). The tissue PCR Kit was obtained from Sigma Aldrich (St. Louis, MO, USA). Primers were purchased by Sigma Aldrich (St. Louis, MO, USA).

2.2. Preparation of CS leaf extract-modified AuNPs

The aqueous stock solutions of CS leaf extract were prepared by mixing 100 mg of extract in 100 ml ultrapure water. The filtered leaf extract, which had a one-week shelf life, was kept at −15 °C for later use. By adding 25 ml of a 1 mM HAuCl4 solution to an oil bath that had been heated to 600 °C while gently mixing it with a hot plate, gold nanoparticles were created. The 25 ml of extract mixture was added to the $HAuCl_4$ solution and kept stirring till 15 min. Finally, 100 μL of 0.1 M ascorbic acid was added to the mixture and the color was turned into red (CS-AuNPs). The CS-AuNPs were centrifuged and characterized with the aid of FTIR, and SEM-EDAX analysis (Katircioğlu et al., 2014). The aqueous extract was preferred to other extracts as they are rich in phenolic and antioxidant ingredients and served for AuNP synthesis that was done in the aqueous environment.

2.2.1. Characterization

Morphologic characterization of modified electrodes was conducted with Field Emission Scanning Electron Microscopy (FEI Quanta 450) operated at secondary electron mode. The crystalline structure of composite electrodes was recorded with the aid of a PANalytical Empyrean diffractometer using Ni-filtered CuKα radiation (λ=1.54050 Å; 45 kV and 40 mA) at room temperature. The Attenuated total reflectance (ATR)-FTIR spectrum of the Au nanoparticle samples was recorded in the wavenumber range of 4000–400 cm^{-1} with Thermo Nicolet 6700 spectrophotometer at 4 cm^{-1} resolution.

2.3. Animals and ethical consideration

In the beginning, 48 male BALB/c mice 6 months old (weighing 18–20 g) were kept in standard conditions (24 ±1°C with a 12–12 h reverse lighting cycle) with unrestricted access to food and water. All experimental protocols were applied following the standards assigned by the Institutional Animal Care and Use Committee at Ataturk University (Decision number E-42190979–000–2200182669, dated 20.06.2022).

2.3.1. Experimental protocol

Six experimental groups each consisting of eight mice were formed: Control group (C), sodium arsenite (As) group, As+10 μg/g AuNPs treated group (As + AuNPs), As+1.6 g/kg CS (As+CS), As+10 μg/g CS-AuNPs treated group (As + CS-AuNPs). Animals were treated with p.o with 10 mg/kg/day As for 21 days (Foyzun et al., 2022a). Treatment of AuNPs and CS-AuNPs continued up to 21 days simultaneously with As administration and all administrations were performed by gavage. The dose of As (10 mg/kg/day) (Foyzun et al., 2022a) and dose of AuNPs (10 μg/g) were selected based on previously reported studies. The dose of CS was selected based on a our previously reported study (Cicek et al., 2022).

2.4. Assessment of behavioral activity

2.4.1. Testing locomotor activity (LAT) in the open-field test

The LAT cage (May 9908, Comment Ltd, Ankara, Turkey) was employed to assess motor deficits caused by arsenic. The test was carried out conforming to previous studies (Cicek et al., 2022). LAT chambers (42 cm L× 42 cm W × 30 cm H) were surrounded by infrared beams, activity was determined as the count of beam deductions (crossings) recorded by a computer and recorded as total distance (cm) and resting time (%) throughout 10 min. During each interval between the phases of experiments, the open field chambers were cleaned with %75 alcohol to remove odors left by the former occupants.

2.4.2. Morrish water maze

The Morrish Water Maze (MWM) test was performed in a circular water tank with a diameter of 150 cm and a depth of 60 cm with an escape platform (10 cm in diameter) 2 cm beneath the water surface. Various visual cues were placed in the water tank, which was artificially separated into four quadrants (i.e., N, E, S, and W), as a sign of space perception. The aim of the training period, which lasted over five days, was for the mice to explore the escape platform by swimming using visual cues within 90 seconds. To determine spatial memory, we used escape latency, swimming speed (cm/s), and distance (cm) which were enrolled by the camera. On Day 6, we conducted a spatial probe trial in which the hidden platform was removed and let the mice swam for 30 seconds. Findings were quantified with Ethovision (Noldus) (Medda et al., 2020).

2.5. Tissue processing

After the behavioral tests, mice were anesthetized with sevoflurane. The hippocampus was surgically removed. The hippocampus samples were taken at −80 °C for biochemical analysis and RNA stabilization reagent for genetic analysis.

2.6. Estimation of oxidative stress

Superoxide dismutase (SOD), glutathione (GSH), and malondialdehyde (MDA) were determined in hippocampal tissue by ELISA kits (Elabscience, Texas, USA) as previously described (Cicek et al., 2023). Hippocampal tissue was homogenized (1000 rpm for 2 minute, QIAGEN TissueLyser II, USA), 50 μL of sample and 50 μL of biotinylated Detection Ab working solution were added to the well and incubated for 45 min at 37 °C. Horseradish peroxidase (HRP) conjugate working solution was put into wells and incubated for 30 min at 37 °C. Then the plate was washed and was added 90 μL substrate reagent. Finally, stop solution was added and the plate was measured at 450 nm using the Multiskan™ GO Microplate Spectrophotometer reader (Thermo Scientific, Canada, USA). Total Oxidant Status (TOS) were determined in hippocampal tissue by ELISA kits (Rel Assay Diagnostics, Gaziantep, Turkey) as specified by manufacturer's directions (Erel, 2005). The absorbance of TOS was determined at 630 nm and 590 nm respectively with a microplate reader.

2.7. Estimation of pro-inflammatory cytokine

Homogenates of the hippocampus were used for measuring TNF-α and IL-1β level by using ELISA kits (Elabscience, Texas, USA) following the manufacturer's guidelines. In a nutshell, the samples (100 L) were added to the wells and allowed to incubate for 90 minutes at 37 °C. Working solutions for biotinylated detection ab were added and incubated for 60 minutes. The plate was then washed, 100 μL of the working horseradish peroxidase (HRP) conjugate solution was added, and it was incubated at 37 °C for 30 minutes. The Multiskan™ GO Microplate Spectrophotometer reader (Thermo Scientific, Canada, USA) was then used to measure the optical density (OD) at 570 nm after the addition of 90 μL of substrate reagent and 50 μL of stop solution, respectively.

2.8. Estimation of apoptotic markers

Homogenates of the hippocampus measuring of Bax, Bcl-2 and caspase-3 were done by using ELISA kit (Elabscience, Texas, USA). The concentrations of Bax, Bcl-2 and caspase-3 were determined in line with previously published protocols (Cicek et al., 2022). Wells with the appropriate volume of samples were filled, and the samples were then incubated at 37 °C for 90 min. After removing the liquid, each well received a dose of biotinylated detection Ab working solution before being properly incubated. The operating solution is HRP conjugate. After the substrate solution had been incubating for 15 minutes, the stop solution was added. The Multiskan™ GO Microplate Spectrophotometer reader (Thermo Scientific, Canada, USA) was used to measure OD at 570 nm.

2.9. Estimation of dopamine receptors

2.9.1. Hippocampal tissue mRNA extraction and cDNA synthesis

RNA Stabilization Reagent (RNAlater™, QIAGEN Hilden, Germany) was used to stabilize the hippocampal tissue samples before they were disrupted with the Tissue Lyser II (2×2 min, Qiagen). Using the RNA easy Mini Kit Qiagen and adhering to the manufacturer's instructions, total RNA was purified. Using a cDNA Reverse Transcription Kit (Applied Biosystems, CA, USA), the RNA samples were reverse-transcribed into complementary DNA. 10 μL of total RNA, 2 μL of 10 RT random primers, 2 μL of 10 RT buffer, 1 μL of MultiScribe reverse transcriptase, 4.2 μL of $DEPCH_2O$, and 0.8 μL of 25 dNTPs mix were combined. Using a Veriti 96-well thermal cycler from Applied Biosystems, reverse transcription was carried out at 25 °C for 10 min, 37 °C for 120 min, and then 85 °C for 5 min. Nanodrop spectrophotometry was used to assess the quality of the obtained cDNA (EPOCH Take 3 Plate, BioTek).

2.9.2. Real-time quantitative PCR analyses

Rotor-Gene Q (QIAGEN) was used to conduct relative D1 and D2 expression analyses in hippocampal tissue. For PCR amplification, TaqMan Gene Expression Assays for mice D1 and for mice D2 (Applied Bio-systems) were utilized. Each 20 μL reaction for each sample contained three triplicate reiterations with 9 μL of cDNA (100 ng), 10 μL of QuantiTect Probe PCR Master mix, and 1 μL of Primer Perfect Probe mix from Qiagen, Hilden, Germany. After being heated for 2 minutes at 50 °C and 10 minutes at 95 °C, the samples underwent 40 cycles of 15 seconds at 94 °C and 60 seconds at 60 °C. The house-keeping gene β -actin was used, and the $2^{-\Delta\Delta}$Ct method was used to normalize the relative expressions of each protein to β-actin. Table 1 displayed each primer sequence.

2.10. Statistical analysis

The SPSS 20.00 program (SPSS Inc., Chicago, IL, USA) was used for all statistical analyses. Both normality and homogeneity were assessed using the Shapiro-Wilk and Levene tests. One-way ANOVA was used to compare the groups, and then Tukey's post hoc test was run. P-values lower than 0.05 were regarded as statistically significant. Results were shown as means with standard deviations (SD).

Table 1
Sequence list of the primers used for RT-PCR.

Genes	Forward Sequence (5′-3′)	Reverse Sequence (3′-5′)
D1	5′-ACCGGAAGTGCTTTCCTTCTG GA-3′	5′-TAGCGGCTGAAGCACTGCA-3
D2	5′-GAGGAAGCATGCCTTGAA AA-3′	5′TGGTGCAGATGAACTTCAGG-3′

3. Results

3.1. Morphological characterization

Field Emission Scanning Electron Microscopy (FESEM) images disclosed that aqueous solution of CS leaf extract influence the morphology of growth of AuNPs. The interconnected quasi spherical shape of AuNPs with the particle size of 55–70 nm, which were obtained without addition of artichoke, can be seen in FESEM images (Fig. 1A and C). On the other hand, approximately evenly distributed quasi-spherical gold nanoparticles with sizes of 20–35 nm were obtained in the presence of CS leaf extract (Fig. 1B and D). The EDX results (Fig. 1E) indicate the presence of carbon, nitrogen, and oxygen on the surface of gold nanoparticles synthesized in the presence of the CS extract.

3.2. XRD studies

The crystallographic structure of synthesized AuNPs were examined with X-ray diffractometer, and the obtained results were given in Fig. 2. The peaks at 37.56, 44.30, 64.27, and 77.31 are attributed to Bragg reflections (111), (200), (220), and (311) of face center cubic (fcc) lattice of AuNPs (Biao et al., 2018).

3.3. FTIR studies

ATR-FTIR measurements were recorded for the possible binding of phytomolecules to AuNPs. According to the Fig. 3 shows the (ATR)-FTIR spectra of CS leaf extract modified AuNPs. The IR bands observed at 3272 cm^{-1} can be attributed to OH stretching vibrations (of water,

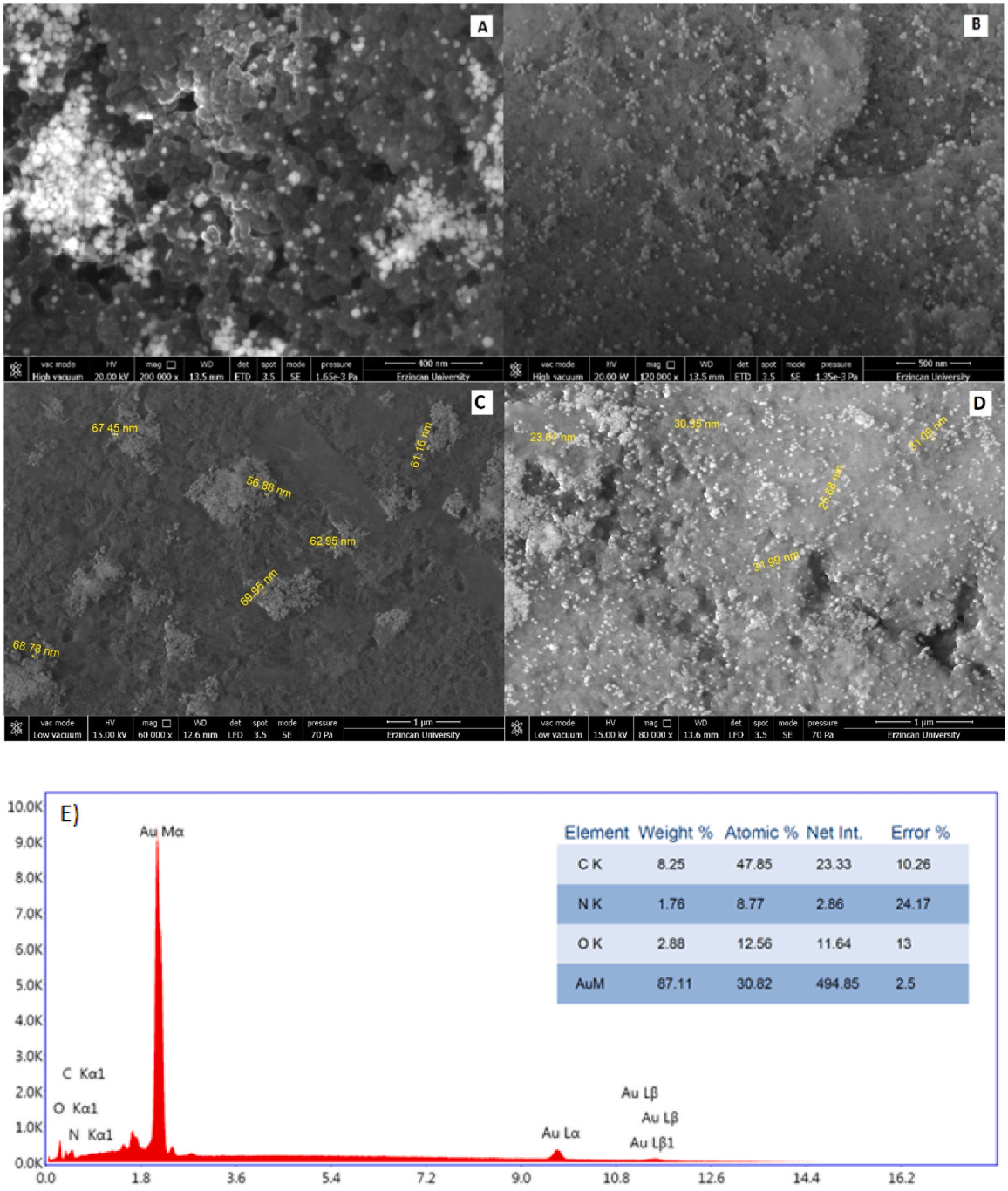

Fig. 1. FESEM images (A), (C) of AuNPs (B),(D) Cs- AuNPs (E) EDX spectrum of Cs-AuNPs. CS-AuNPs: C. scolymus leaf mediated gold nanoparticles (AuNPs).

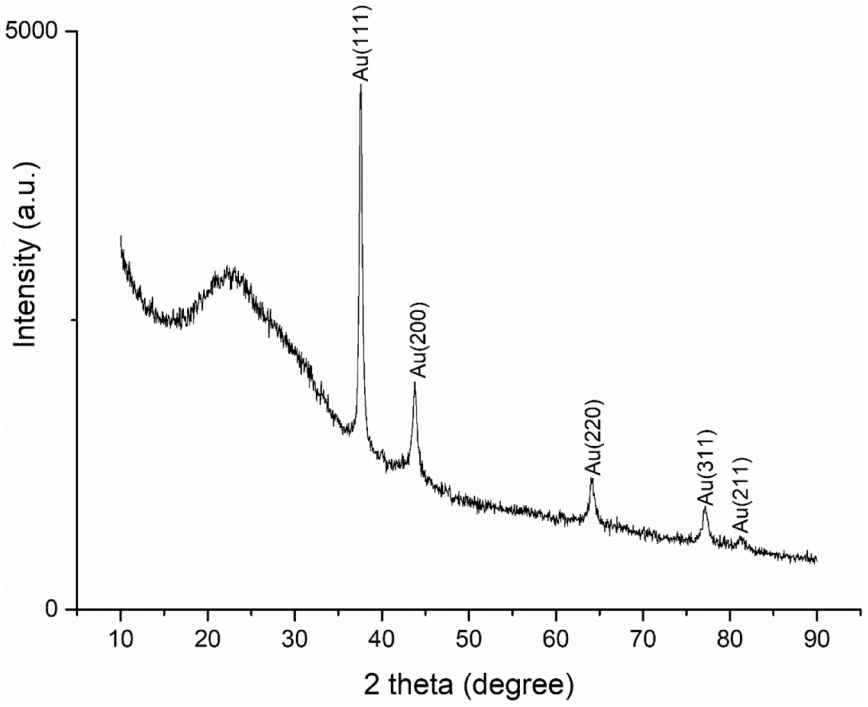

Fig. 2. X-ray diffraction pattern of Cs- AuNPs. CS-AuNPs: C. scolymus leaf mediated gold nanoparticles (AuNPs).

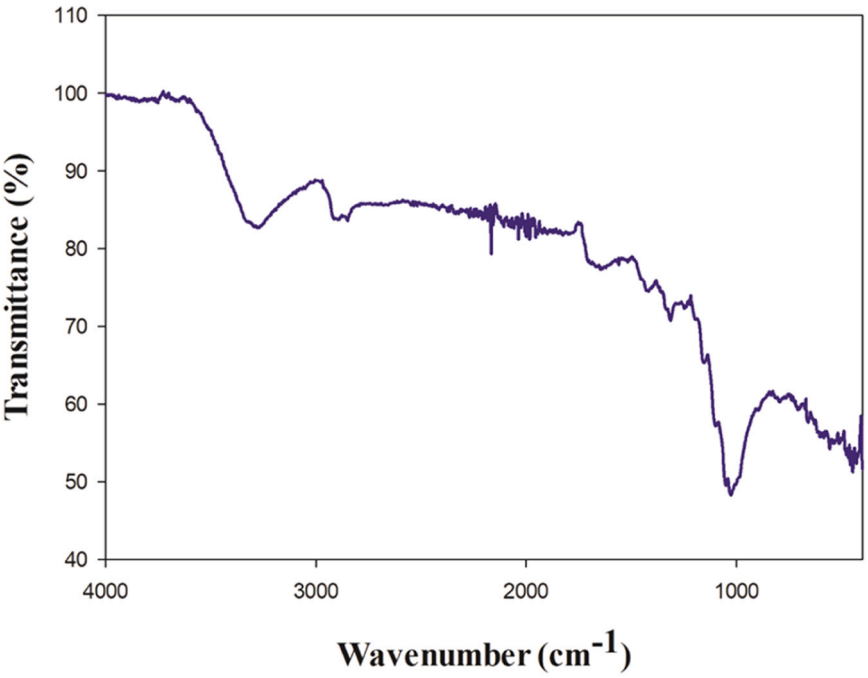

Fig. 3. ATR-FTIR transmittance (%) and wavenumber spectrum of Cs- AuNPs. CS-AuNPs: C. scolymus leaf mediated gold nanoparticles (AuNPs).

alcohols, phenols, carbohydrates, peroxides), while the band at 2848 can be assigned to C–H stretching vibrations. The broad band at 1620–1700 cm^{-1} depicts the carbonyl moieties in the phytochemicals. The peaks at 1400, 1250 and 1020 cm^{-1} can be resulted from C–O (amide) and C–C stretching's from phenyl groups, carbonyl C–O stretching vibrations, C–O–C linkages or C–O stretching from phenolic compounds, respectively (Das et al., 2012). Due to the obtained results, it is clearly seen that the CS leaf extract was bonded to AuNPs surface. These results also were good agreement with EDX results

3.4. CS-AuNPs improved motor behavior in As-treated mice

Open-field activity tests were performed to evaluate the CS-AuNPs effects on locomotor performance. We observed that total traveled distance (2193.25 ± 140.22 cm, $p<0.001$) was significantly reduced while resting time was significantly (62.87% ± 1.09 cm, $p<0.001$) increased in As-treated mice when compared to the control group (6949 ± 310.7 cm, %32.98 ± 1.98; respectively) (Fig. 4A-B). The reduction in total travel distance and increase in resting time induced by As was restored partially by CS treatment (4121.78 ± 147.3 cm, %41 ± 2.14,

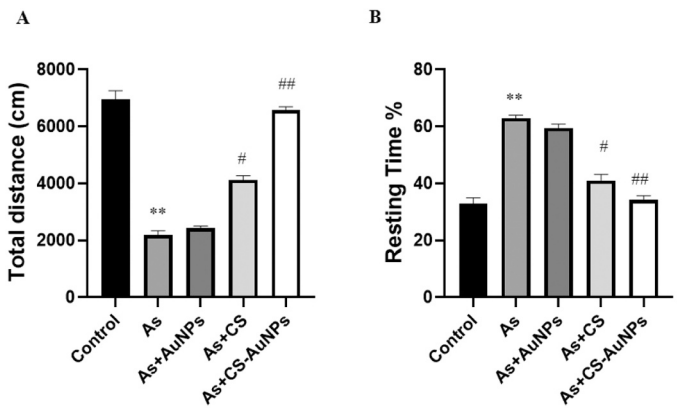

Fig. 4. Behavioral alterations of CS-AuNPs -treated mice in the LAT test. (A) Total distance covered in LAT. (B) Resting time in LAT. Data are presented as the means ± SD * $p<0.05$, ** $p<0.001$, vs. control group, # $p<0.05$, ## $p<0.001$ vs. As group. As group. As: Sodium arsenite, AuNPs: Gold nanoparticles, CS: C. scolymus leaf extract, CS-AuNPs: C. scolymus leaf mediated gold nanoparticles.

$p<0.05$; respectively); whereas, this was reversed completely in mice that received CS-AuNPs treatment (6579.41 ± 112.78 cm, %34.26 ± 1.46, $p<0.001$; respectively). In contrast, 10 μg/g AuNP treatment did not alter the reduction in As-induced total distance and the increase in resting time ($p>0.05$).

3.5. CS-AuNPs improved cognitive function in As-treated mice

To assess the effect of CS-AuNPs treatment on the learning and memory functions in the mice, the MWM was employed. We found that the animals in the As group spent more time finding the hidden platform from the 3th day compared with the animals in the control group in the training period; however, the treatment with CS ($p<0.05$) and CS-AuNPs reduced learning latency ($p<0.001$). On the other hand, the animals in the CS-AuNPs group showed learning latency similar to that of control mice (Fig. 5A). During the probe test, the animals in the As group (23 ± 1.41 sn; $p<0.001$) showed poor memory retention, spent less time in the target quadrant compared to the animals in the control (77 ± 1.73 sn). The learning and memory impairment induced by As was significantly reversed by CS treatment (53 ± 3.16; $p<0.05$). The mice that received CS-AuNPs treatment remembered the previous platform location better and exhibited more time in the target quadrant (81 ± 2.56; $p<0.001$) (Fig. 5B). In contrast, 10 μg/g AuNP treatment did not alter the escape latencies and time spent in the target quadrant ($p>0.05$).

3.6. CS-AuNPs reduced oxidative stress and improved antioxidant level in As-treated mice

To assess the effect of CS-AuNPs on oxidative stress in the hippocampus, we measured the levels of SOD, GSH, MDA and TOS (Fig. 6). Compared to the control animals hippocampus' SOD and GSH levels (7.49 ± 0.19 U/mg protein, 7.8 ± 0.33 nmol/mg protein, respectively) were reduced significantly (2.12 ± 0.11 U/mg protein, 3.8 ± 0.21 nmol/mg protein, respectively) in mice treated with As. The decreased SOD and GSH levels in As-treated mice were improved partially by CS treatment (3.98 ± 0.29 U/mg protein, 5.23 ± 0.34 nmol/mg protein, $p<0.05$, respectively); whereas, they were restored completely by the administration of CS-AuNPs (6.87 ± 0.23 U/mg protein, 7.00 ± 0.03 nmol/mg protein, $p<0.001$, respectively).

We measured MDA levels, indicator of lipid peroxidation and oxidative stress, in hippocampus tissue. As treatment significantly increased the MDA levels (9.76 ± 0.3 nmol/mg protein; $p<0.001$) in the hippocampus compared to control mice levels (4.04 ± 0.24 nmol/mg protein). In addition, we also measured TOS levels, another biochemical parameter supporting oxidative stress, in the hippocampus. TOS is used to determine the cumulative oxidative effects of various oxidants in biological systems (Erel, 2005). Compared to the control mice (4.31 ± 0.77 μmolH_2O_2 Equiv/L), TOS level was increased marked (16.09 ± 0.81 μmolH_2O_2 Equiv/L, $p<0.001$) in mice treated with As. The elevated hippocampus levels of MDA and TOS in As-treated mice were alleviated relatively by CS treatment (6.47 ± 0.13 nmol/mg protein, 9.00 ± 0.4 μmolH_2O_2 Equiv/L, $p<0.05$, respectively); however, they were further restored by the administration of CS-AuNPs (4.28 ± 0.81 nmol/mg protein, 5.31 ± 0.21 μmolH_2O_2 Equiv/L, $p<0.001$, respectively). On the other hand, the application of 10 μg/g AuNP did not affect the oxidative stress parameters including SOD, GSH, MDA, and TOS in the hippocampus compared to As-induced mice ($p>0.05$).

3.7. CS-AuNPs administration limited hippocampal inflammation in As-treated mice

We explored the mechanism of CS-AuNPs neuronal protection during As neurodegeneration in the hippocampus by measuring TNF-α and IL-1β protein levels. In As-treated mice, TNF-α (5.46 ± 0.24 pg/mg protein, $p<0.001$) and IL-1β (1.72 ± 0.21 pg/mg protein, $p<0.001$) were significantly increased in the hippocampus as compared to control mice (1.58 ± 0.47 pg/mg protein, 0.54 ± 0.16 pg/mg protein, respectively) (Fig. 7A-B). The elevated TNF-α and IL-1β levels in As-treated mice were alleviated partially by CS treatment (3.25 ± 0.20 pg/mg protein, 0.9 ± 0.10 pg/mg protein, $p<0.05$, respectively); however, they were restored completely by CS-AuNPs treatment (2.10 ± 0.26 pg/mg protein, 0.69 ± 0.31 pg/mg protein, $p<0.001$, respectively). In contrast, 10 μg/g AuNP

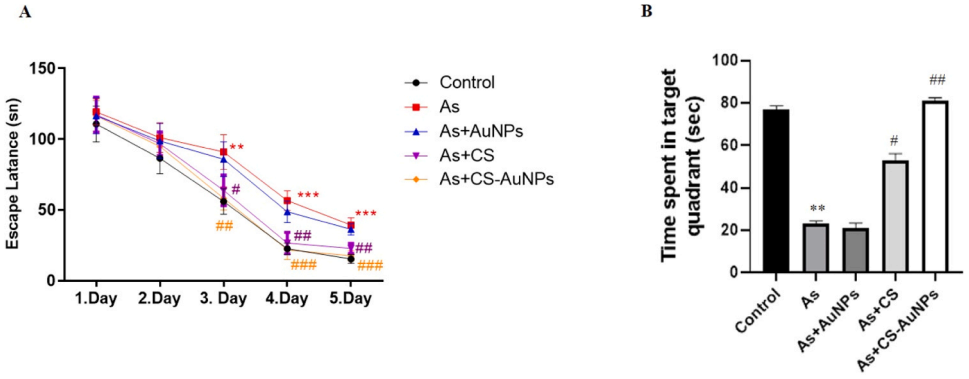

Fig. 5. Effects of CS-AuNPs on As-induced spatial memory impairment. (A) Escape latency to find the platform during the training stages. (B) The time spent in target quadrant of probe trial. Data are presented as the means ± SD * $p<0.05$, ** $p<0.001$, vs. control group, # $p<0.05$, ## $p<0.001$ vs. As group. As: Sodium arsenite, AuNPs: Gold nanoparticles, CS: C. scolymus leaf extract, CS-AuNPs: C. scolymus leaf mediated gold nanoparticles.

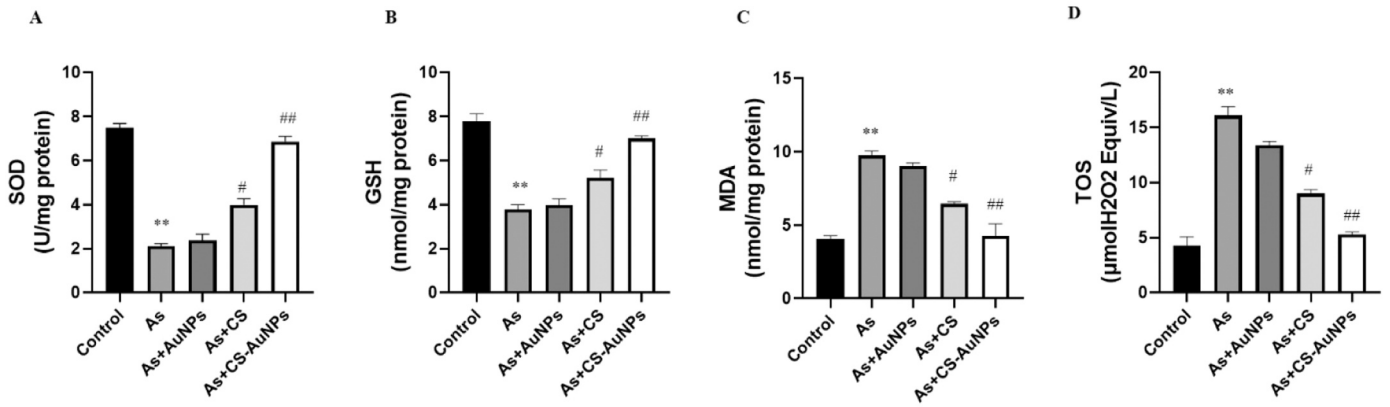

Fig. 6. Oxidative stress markers in hippocampus. (A) SOD (B) GSH (C) MDA and (D) TOS levels. Data are presented as the means ± SD *p<0.05, **p<0.001 vs. control group, # p<0.05, ##p<0.001 vs. As group. As: Sodium arsenite, AuNPs: Gold nanoparticles, CS: C. *scolymus* leaf extract, CS-AuNPs: C. scolymus leaf mediated gold nanoparticles.

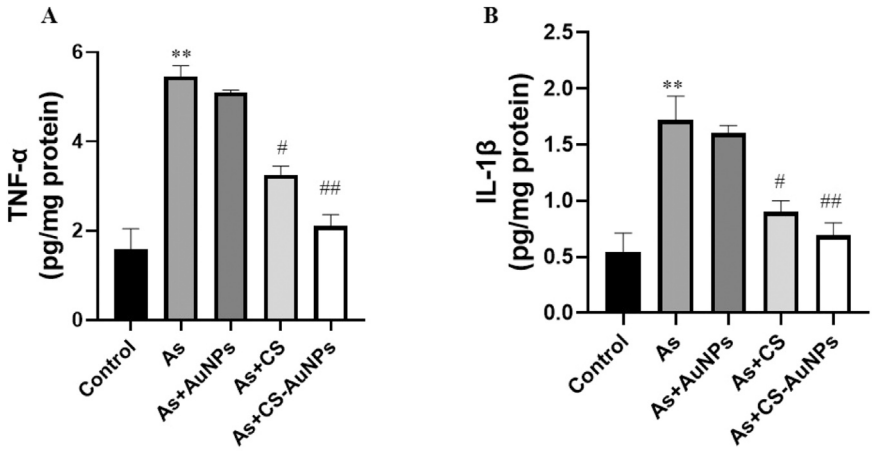

Fig. 7. Inflammatory markers in hippocampus. (A) TNF-α (B) IL-1β. Data are presented as the means ± SD *p<0.05, **p<0.001 vs. control group, # p<0.05, ##p<0.001 vs. As group. As: Sodium arsenite, AuNPs: Gold nanoparticles, CS: C. scolymus leaf extract, CS-AuNPs: C. scolymus leaf mediated gold nanoparticles.

treatment did not change the As-induced inflammation in the hippocampus (p>0.05) (Fig. 7). These findings suggest CS-AuNPs inhibited the production of inflammatory mediators, indicating their anti-inflammatory role.

3.8. CS-AuNPs inhibited hippocampal neuronal apoptosis by increasing the Bax/Bcl-2 ratio and inhibited caspase-3 activation

In order to explore the mechanisms of the antiapoptotic effects of CS-AuNPs against neurodegeneration in the hippocampus, we measured the Bax and Bcl-2 protein levels. In As-treated mice, Bax level (23.39 ± 1.5 ng/ml, p<0.001) was significantly increased, while Bcl-2 level (6.24

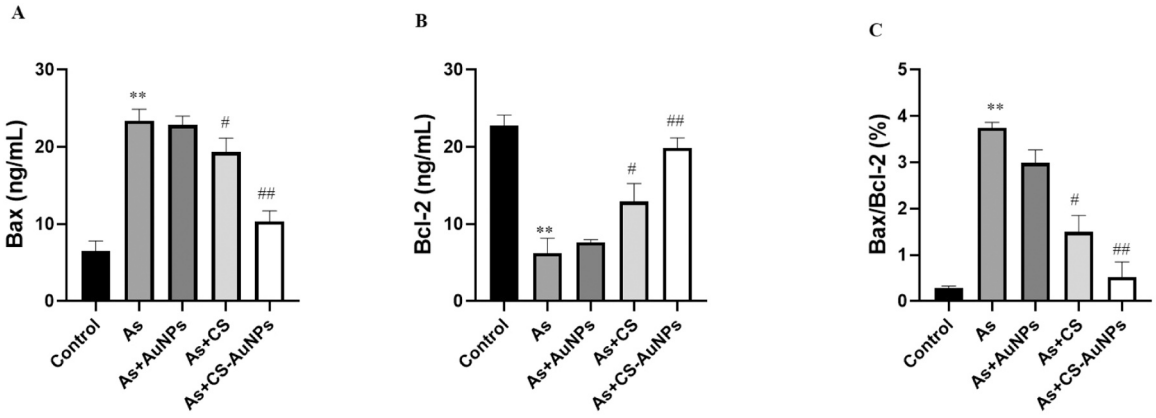

Fig. 8. Apoptotic markers in hippocampus. (A) Bax (B) Bcl-2 (C) Bax/Bcl-2. Data are presented as the means ± SD *p<0.05, **p<0.001 vs. control group, # p<0.05, ##p<0.001 vs. As group. As: Sodium arsenite, AuNPs: Gold nanoparticles, CS: C. scolymus leaf extract, CS-AuNPs: C. scolymus leaf mediated gold nanoparticles.

± 1.92 ng/ml, p<0.001) was significantly decreased in the hippocampus compared to control mice (6.5 ± 1.32 ng/ml, 22.8 ± 1.35 ng/ml) (Fig. 8A-B). CS treatment in As-treated mice partially reduced Bax protein levels (19.32 ± 1.85 ng/ml, p<0.05), while relatively enhanced Bcl-2 levels (12.91 ± 2.34 ng/ml, p<0.05) in the hippocampus compared with As-treated mice. However, the most prominent therapeutic effect was detected in CS-AuNPs treated animals. Bax (10.34 ± 1.4 ng/ml, p<0.001) and Bcl-2 (19.88 ± 1.3 ng/ml, p<0.001) levels were restored completely by the CS-AuNPs administration (Fig. 8A-B). Compared to the control mice (0.28% ± 0.04), Bax/Bcl-2 ratio (3.75% ± 0.12, p<0.001) was increased significantly in the hippocampus in mice treated with As (Fig. 8C). The As-induced elevation in Bax/Bcl-2 ratio was reduced relatively by CS treatment (1.5% ± 0.36, p<0.05); whereas, it was decreased significantly in mice that received CS-AuNPs (0.52% ± 0.33, p<0.001). These findings indicated that treatment with CS-AuNPs diminished the increase in Bax level and enhanced the level of Bcl-2, leading to an increase in the Bcl-2 to Bax ratio. These results demonstrated that CS-AuNPs inhibit neuron apoptosis in As-treated animals by decreasing the Bax/Bcl-2 ratio in the hippocampus.

To further elaborate our study and to examine whether the neuroprotective effect of CS-AuNPs is also related to the inhibition of As-treated apoptotic response, we measured protein levels of caspase-3 in the hippocampus. Compared to the control mice (2.70 ± 0.02 ng/ml), the caspase-3 protein level was increased significantly (11.54 ± 0.42 ng/ml, p < 0.001) in the hippocampus of As-treated mice (Fig. 9). The As-induced elevation in caspase-3 protein level was reduced partially by CS treatment (6.20 ± 0.8 ng/ml, p<0.05); whereas, it was diminished completely in mice received CS-AuNPs treatment (3.88 ± 0.43 ng/ml, p<0.001). In contrast, 10 μg/g AuNP treatment had no effect on the As-induced alteration of apoptotic markers in the hippocampus (p>0.05).

3.9. D1 and D2 receptors both mediated the protection of CS-AuNPs on spatial memory of As-induced neurotoxicity

We investigated whether CS-AuNPs treatment could restore spatial learning and memory. Therefore, to indicate that improved cognitive functions upon CS-AuNPs treatment were actually dependent on the DA receptors, we examined the D1 and D2 receptor mRNA expressions in the hippocampus. There was a significant reduction in mRNA expression of D1 (0.31± 0.03 fold, p<0.001) and D2 (0.6 ±0.02 fold, p<0.001) receptors in the hippocampus of As-treated mice compared to control mice (Fig. 10A-B). The As-induced reduction in D1 and D2 receptor mRNA expressions were restored partially by CS treatment (0.53± 0.07fold, 0.76± 0.01fold, p<0.05, respectively); whereas, their mRNA expression was recovered completely in mice treated with CS-AuNPs

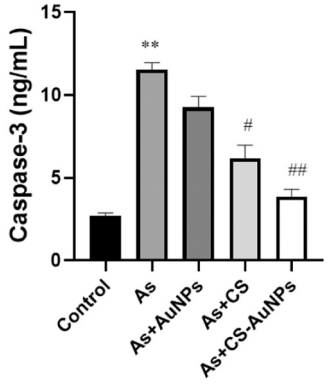

Fig. 9. Caspase-3 level in hippocampus. Data are presented as the means ± SD *p<0.05, **p<0.001 vs. control group, # p<0.05, ##p<0.001 vs. As group. As: Sodium arsenite, AuNPs: Gold nanoparticles, CS: C. scolymus leaf extract, CS-AuNPs: C. scolymus leaf mediated gold nanoparticles.

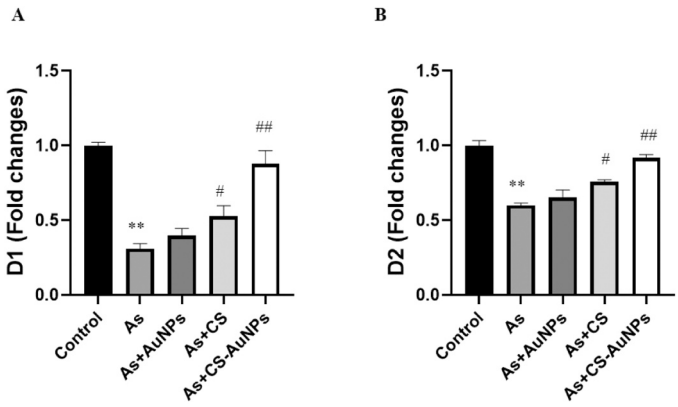

Fig. 10. (A) D1 and (B) D2 expression levels in hippocampus. Data are presented as the means ± SD *p<0.05, **p<0.001 vs. control group, # p<0.05, ##p<0.001 vs. As group. As: Sodium arsenite, AuNPs: Gold nanoparticles, CS: C. scolymus leaf extract, CS-AuNPs: C. scolymus leaf mediated gold nanoparticles.

(0.89 ± 0.09 fold, 0.92± 0.02 fold, p<0.001, respectively). However, 10 μg/g AuNP administration had no significant effect on D1 and D2 receptors mRNA expression when compared to the As-treated group (p>0.05).

4. Discussion

The formation of interconnected quasi-spherical gold nanoparticles in the absence of CS leaf extracts indicates the development of flocculation in the system, which promotes the formation of coagulation structures (Fig. 1A and C). On the other hand, in the presence of CS leaf extract, the formation of uniformly distributed individual gold nanoparticles was observed (Fig. 1B and D). The latter effect may be due to the adsorption of phytocomponents with the formation of a shell that sterically and electrostatically stabilizes gold nanoparticles. Thus, as a result of the adsorption of phytocomponents of the CS leaf extract, the flocculation of gold nanoparticles is suppressed. The presence of adsorption of biogenic molecules on the surface of gold nanoparticles is evidenced by the EDX (Fig. 1E) and FTIR (Fig. 3) data. On the other hand, quasi-spherical gold nanoparticles obtained in the presence of phytocomponents have a size of 20–35 nm and are much smaller than gold nanoparticles formed in the absence of CS leaf extracts (55–70 nm). Consequently, phenolic compounds, flavonoids, and tannins contained in the CS leaf extract (Cicek et al., 2022; Ibrahim et al., 2022) affect not only the colloidal stability of nanoparticles, preventing their flocculation, but also affect the growth processes of new phase nuclei. It is likely that the adsorption of phytocomponents limits the growth of new phase nuclei by interrupting the diffusion flow from the supersaturated solution.

By themselves, nanomaterials such as multi-walled carbon nanotubes have the ability to reduce the cognitive abilities in Wistar rats (Sayapina et al., 2016) but at the same time they are capable carriers and provide an efficient delivery system for different drugs (Kuskov et al., 2022). Nanoparticles' physicochemical properties are the main determinant of their effectiveness in drug delivery and function regarding human physiology. Their surface charge, particle size, and chemical composition can strongly affect NPs concentration in different organs and determine the likelihood to cause increased production of reactive oxygen species (ROS) and thus by themselves inflict tissue oxidative damages (Bostan et al., 2016). However, specific nanocarriers such Amphiphilic poly-N-vinylpyrrolidone nanoparticles, despite their effectiveness in penetrating human microvascular endothelial cells, do not activate vascular endothelium and affect its viability at pharmacological relevant concentrations (Berdiaki et al., 2022). Gold nanoparticles especially are thought to be highly biocompatible compared to

other metallic nanoparticles and offer a number of advantages such as controlled synthesis, increased targeting properties, and the ability to transport large amounts of loaded drugs (Mioc et al., 2018). Gold nanoparticles are favored by their inert nature and their potential to bind to multiple surface ligands allowing them to penetrate cells and function without provoking significant immune response. However, AuNPs interactions depend on their NPs size. It is known that AuNPs of 20 nm (AuNP20) could be internalized in cytosolic vacuoles, whilst AuNP70 are restricted to the cell membrane (Engin et al., 2017).

Arsenic is a major environmental pollutant with multiple toxic effects on human populations and arsenic contamination is becoming an environmental health problem worldwide. Of all organs, the brain is the most sensitive to the toxic effects of arsenic. Many reports have shown that arsenic traverses the blood-brain barrier, affecting brain functions, causing learning impairment and behavioral abnormalities (Xiong et al., 2021). In this study we used a mice model of arsenic-induced neurobehavioral deficits to evaluate the protective effects of AuNPs with Cynara scolymus leaf extracts. The animals were 6 months old which is equivalent to 30 years old humans (Flurkey et al., 2007). The design of the animal study used adult mice in order to prevent signs of ageing in the central nervous system. Moreover, male mice were chosen because they are used extensively in animal testing and have less variability compared to females, which have estrous cycles - a faster version of the human menstrual cycle that determines the change in hormone concentration on a four or five-day schedule, so if female mice are at different points in their estrous cycle, their response can vary too widely (Zucker and Beery, 2010). Regarding the doses of Arsenic used in this model, even if low doses of around 4 mg/kg showed mitochondrial toxicity in hippocampal cells, for the evaluation of behavioral changes induced by arsenic, chronic exposure is needed, and previous studies showed that chronic exposure to 10 mg/kg bw induces behavioral changes, oxidative stress and apoptosis, without lethality (Foyzun et al., 2022b; Goudarzi et al., 2018). This study reported that As-treated mice exhibited in the hippocampus significant oxidative-inflammatory stress, apoptosis, decreased expression of D1 and D2, and ultimately decrease in locomotor activity with cognitive alterations, which were evaluated by biochemical, molecular, LAT and WMW analyses. Our findings showed that the CS leaf extract-associated AuNPs produced by the green synthesis method have a superior protective effect compared to free CS against As-induced hippocampal toxicity by mitigating oxidative damage, inflammation, apoptosis, D1 and D2 receptor alterations, whilst suppressing the behavioral changes induced by As. Drug delivery to brain lesions should consider and overcome some brain-specific issues such as the precise physiological brain homeostasis and the great vulnerability of the neurons. Nanoparticles are ideal for brain drug delivery because they are not limited to the systemic circulation and can cross the blood–brain barrier (BBB) contrary to many other therapeutic preparations. Nanocarriers offer also the option of CNS-targeted drug availability (Henrich-Noack et al., 2019).

Numerous studies have demonstrated that exposure to arsenic promotes hippocampal degeneration, inducing cognitive and learning deficits (Mehta et al., 2021; Pandey et al., 2022; Wang et al., 2021). The variability in the plastic nature of the hippocampus is one of several factors that determine its vulnerability to numerous insults (Dixit et al., 2020). Hippocampus is a region of great interest due to its involvement in cognitive ability and motor activity (Burman, 2019). In our study, we reported that As-treated mice displayed longer swimming latency and shorter duration in the target quadrant in the MWM task, suggesting impairment in the learning and memory induced by As. Also, in mice intoxicated with As, the impairment of locomotor and investigative functions was manifested by LAT findings. Data from other animal studies are congruent and support our findings of As-induced cognitive and motor impairment (Kumar et al., 2013; Rodrıguez et al., 2002). CS-AuNPs ameliorated the degenerative effects of As on the CNS and led to a noticeable improvement in performance and recovery in cognitive abilities. At the same time, the current study found that CS treatment can ameliorate As-induced behavioral changes but cannot completely reverse them. Surprisingly, discrete AuNPs treatment did not ameliorate behavioral deficits. In the literature, there are no reports regarding AuNPs or CS effects in As-induced behavioral alterations. On the other hand Hou et al. (2020) previously reported that the chiral AuNPs can reverse memory deficits in a mouse model of Alzheimer's disease (Hou et al., 2020). Also Xue et al. demonstrated that administration of AuNPs synthesized using *Paeonia mountan* improved the motor coordination in Parkinson's disease induced mice (Xue et al., 2019).

The cognitive and motor dysfunction of As-intoxicated mice is closely linked to the hippocampal neuronal damage that results from the excessive production of free radicals that eventually cause oxidative stress (Medda et al., 2020; Xiong et al., 2021). In the present report, oxidative damage with impaired redox balance was observed in the hippocampi of As-exposed mice evident by a remarkable elevation in MDA and TOS levels associated with a reduction in SOD and GSH levels. Following the elevated lipid peroxidation and the inhibition of the enzymatic and non-enzymatic antioxidant activity of mice exposed to As, the antioxidant/pro-oxidant ratio is disturbed and eventually oxidative stress is induced. Our results were compatible with those of previous studies which demonstrated that oxidative stress plays the main role in As-induced brain damage and cognitive impairment (Sharma et al., 2018; Taheri Zadeh et al., 2021). CS and especially CS-AuNPs treatment led to an improvement of oxidative stress markers. Recent studies on the effects of herbal plant AuNPs *in vivo* disease models such as Parkinson's disease (PD), and radiation-induced brain damage in rats have supported the idea that these nanoparticles are capable of ameliorating harmful free radicals and thus protecting the brain against oxidative stress-induced neurodegeneration (Abdelkader et al., 2022; Subakanman et al., 2015).

Recent studies have proposed that As-induced oxidative damage is mediating inflammation in the hippocampus which in turn is associated with cognitive and neuronal dysfunction in rodent models (Firdaus et al., 2018; Jing et al., 2022). Reduced activity of the antioxidant enzymes and elevated MDA levels in mice exposed to As result in the activation of different pro-inflammatory cytokines including IL-1β, TNF-α, and IL-6 (Firdaus et al., 2018; Jing et al., 2022). There is a link between hippocampal inflammation and cognitive impairment, which reflects the suppression of neuronal functions by cytokines (Prieto et al., 2019). Inflammatory or proinflammatory cytokines are interconnected with oxidative stress parameters. ROS activation leads to secrete cytokine and elevated cytokine induces ROS levels respectively. Zha et al. showed that astrocyte and microglial cells in response to elevated TNF-α and IL-1β levels secrete oxidative stress (ROS) parameters like MDA, SOD, and CAT (Zha et al., 2022). Moreover, it has been shown that the reduction of oxidative stress by natural products can protect neuronal cells. In this study, the As markedly elevated the protein levels of inflammatory intermediaries as TNF-α and IL-1β in the murine hippocampus in a similar way to previous studies (Ishaq et al., 2022; Jing et al., 2022). However, TNF-α and IL-1β protein levels were reduced in the hippocampal tissues following CS and CS-AuNPs treatment, suggesting that these compounds can attenuate neuro-inflammation. It is interesting to note that in the present study, CS-AuNPs supplementation demonstrated the most favorable results. In accordance with the current study, Park et al. (Park et al., 2019b) have demonstrated the anti-neuroinflammatory effects of *Ephedra sinica* Stapf extract-capped gold nanoparticles in reducing TNF-α and IL-1β microglia levels. Another study in a mouse PD model reported that gold nanoparticles from *Cinnamomum verum* improved neuronal inflammation along with beneficial effects on oxidative damage (Ling et al., 2019).

Furthermore, arsenic leads to apoptosis as a result of its potential to initiate cell death signaling (Pandey et al., 2017). Flora et al. (2009) showed that arsenic exposure alters mitochondrial activity and disrupts redox homeostasis in the hippocampus, which eventually leads to cell apoptosis. Bax and Bcl-2 which are associated with apoptosis, are members of the Bcl-2 protein family. Bcl-2 is the primary protein that

inhibits cell apoptosis, while Bax is the protein that promotes apoptosis (Cicek et al., 2022). On the other hand, caspase-3 is considered to be an essential executioner of caspase in apoptosis (D'amelio et al., 2010). This study showed that As exposure leads to elevated Bax and caspase-3 and reduced Bcl-2 levels in accordance with previous data (Pandey et al., 2017). Also, He et al. demonstrated that arsenic promotes high Bax and caspase-3 expression and reduces Bcl-2 expression in mouse oligodendroglia cells (He et al., 2021). Accumulating evidence demonstrates a close association between Bax/Bcl-2 levels and neuronal survival (Raghupathi et al., 2003). The Bax/Bcl-2 ratio is considered a critical factor affecting apoptosis (Raghupathi et al., 2003). Furthermore, in the current study, As administration led to an elevated Bax/Bcl-2 ratio which is considered a trigger of apoptosis. Decreased Bax and caspase-3 activity and increased Bcl-2 protein levels protect hippocampal neuron cells from oxidative damage and apoptosis (Firdaus et al., 2018; Pandey et al., 2017). According to the current study findings, CS and CS-AuNP treatment counteracted apoptosis by reducing caspase-3 and Bax levels, and the Bax/Bcl-2 ratio, and increasing Bcl-2 levels. It is noteworthy, that the anti-apoptotic effects were lower in the CS-treated group than in the CS-AuNPs group. In vitro and in vivo models like oxygen and glucose deprivation/reoxygenation in human-derived neuroblastoma cells (Park et al., 2019a) and radiation-caused brain damage in rats (Abdelkader et al., 2022), green synthesis AuNPs were found capable of neuroprotection via regulation of apoptosis-related proteins, as indicated by decreased caspase-3, Bax levels and increased Bcl-2 levels.

It is well known that DA modulates the animal motor activity and cognitive function and is related to the neurotransmission process (Chandravanshi et al., 2019). As exposure in rodents affected the different types of DA receptors such as D1R and D2R leading to motor and cognitive impairment (Chandravanshi et al., 2019; Htway et al., 2021). In the current study, D1R and D2R mRNA hippocampal level reduction was demonstrated in As-intoxicated mice. This finding led to deterioration of the cognitive and locomotion functions in the As group. Previously published studies showed that dopaminergic neuron signaling and its associated behaviors are susceptible to arsenic, which causes neurobehavioral toxicity (Chandravanshi et al., 2016; Htway et al., 2021). In another report, D1R and D2R inactivation with constitutive knock-out mice in the hippocampus indicated impairment of spatial, associative, and episodic-like memory (Chandravanshi et al., 2019; Takeuchi et al., 2016). On the other hand, both upregulation and downregulation of D1R and D2R have been noticed in arsenic-exposed rats, however, these alterations appear to rely on brain region and dose and duration of arsenic exposure (Chandravanshi et al., 2016; Htway et al., 2021). As noted in our study, CS and especially CS-AuNPs treatment increased D1R and D2R mRNA levels in the hippocampus of As-intoxicated mice, improving dopaminergic neurotransmission, which is associated with motor activity and cognitive function.

5. Conclusion

The current study showed, for the first time, that CS and CS-AuNP administration alleviated neurodegeneration and its associated behavioral impairment in the As-exposure mice model. CS-AuNP effects were more prominent compared to single CS treatment. The greater neuroprotective activity of CS-AuNP can be explained by the improved solubility and bioavailability of CS following gold nanoparticles formulation. The neuroprotective effect of CS-AuNP is attributable to hippocampal-specific changes in oxido-inflammatory and apoptotic signaling, as well as its potential effects on D1R and D2R expression. These findings must be addressed cautiously with further studies. Although CS-AuNPs are promising molecules to treat As-induced cognitive impairment, detailed investigation of different molecular pathways needs to be performed. In addition, integrated safety assessment and dose optimization of CS-AuNPs for clinical applications need further research.

Funding

The present study was partly funded by the European Union's Horizon Europe framework program project 'European Partnership for the Assessment of Risks from Chemicals (PARC).

CRediT authorship contribution statement

Ali Taghizadehghalehjoughi, Betul Cicek, Ahmet Hacimuftuoglu, Anca Oana Docea, Aristidis Tsatsakis designed the experiments. Betul Cicek, Ahmet Hacimuftuoglu, Yesim Yeni, Mehmet Kuzucu, Sidika Genc, Ahmet Cetin, Emre Yavuz, Betul Danısman, Akin Levent, Kemal Volkan Ozdokur, Mecit Kantarcı, Vasileios Siokas and Konstantinos Tsarouhas performed the experiments. Aristidis Tsatsakis, Kemal Volkan Ozdokur, Betul Danısman, Vasileios Siokas, Michael D. Coleman, Anca Oana Docea and Konstantinos Tsarouhas analyzed the data. Betul Cicek, Ahmet Hacimuftuoglu, Yesim Yeni, Mecit Kantarcı, Sidika Genc, Ahmet Cetin, Emre Yavuz, Betul Danısman, Akin Levent, Kemal Volkan Ozdokur, Mehmet Kuzucu, Vasileios Siokas and Konstantinos Tsarouhas wrote the first draft of the manuscript. Michael D. Coleman, Anca Oana Docea, Konstantinos Tsarouhas, Akin Levent, Ali Taghizadehghalehjoughi and Aristidis Tsatsakis revised the first draft and finalized the manuscript. All authors have read and approved the final manuscript.

Declaration of Competing Interest

The authors declare that they have no known competing financial interests or personal relationships that could have appeared to influence the work reported in this paper.

Data availability

Data will be made available on request.

References

Abdelkader, N.F., El-Batal, A.I., Amin, Y.M., Hawas, A.M., Hassan, S.H., Eid, N.I., 2022. Neuroprotective effect of gold nanoparticles and alpha-lipoic acid mixture against radiation-induced brain damage in rats. Int. J. Mol. Sci. 23 (17), 9640.

de Bem Silveira, G., Muller, A.P., Machado-de-Ávila, R.A., Silveira, P.C.L., 2021. Advance in the use of gold nanoparticles in the treatment of neurodegenerative diseases: new perspectives. Neural Regen. Res. 16 (12), 2425.

Berdiaki, A., Kuskov, A.N., Kulikov, P.P., et al., 2022. In vitro assessment of Poly-N-vinylpyrrolidone/acrylic acid nanoparticles biocompatibility in a microvascular endothelium model. Int J. Mol. Sci. 23 (20) https://doi.org/10.3390/ijms232012446.

Biao, L., Tan, S., Meng, Q., et al., 2018. Green synthesis, characterization and application of proanthocyanidins-functionalized gold nanoparticles. Nanomaterials 8 (1), 53.

Bostan, H.B., Rezaee, R., Valokala, M.G., et al., 2016. Cardiotoxicity of nano-particles. Life Sci. 165, 91–99. https://doi.org/10.1016/j.lfs.2016.09.017.

Burman, D.D., 2019. Hippocampal connectivity with sensorimotor cortex during volitional finger movements: Laterality and relationship to motor learning. PloS One 14 (9), e0222064.

Cabuzu, D., Cirja, A., Puiu, R., Mihai Grumezescu, A., 2015. Biomedical applications of gold nanoparticles. Curr. Top. Med. Chem. 15 (16), 1605–1613.

Chandravanshi, L.P., Gupta, R., Shukla, R.K., Khanna, V.K., Trigun, S.K., 2016. Perinatal arsenic exposure alters central dopaminergic system of rats. Park. Relat. Disord. 22, e185.

Chandravanshi, L.P., Gupta, R., Shukla, R.K., 2019. Arsenic-induced neurotoxicity by dysfunctioning cholinergic and dopaminergic system in brain of developing rats. Biol. Trace Elem. Res. 189 (1), 118–133.

Cicek, B., Genc, S., Yeni, Y., et al., 2022. Artichoke (Cynara scolymus) Methanolic Leaf Extract Alleviates Diethylnitrosamine-Induced Toxicity in BALB/c Mouse Brain: Involvement of Oxidative Stress and Apoptotically Related Klotho/PPARγ Signaling. J. Pers. Med. 12 (12), 2012.

Cicek, B., Hacimuftuoglu, A., Yeni, Y., et al., 2023. Chlorogenic Acid Attenuates Doxorubicin-Induced Oxidative Stress and Markers of Apoptosis in Cardiomyocytes via Nrf2/HO-1 and Dityrosine Signaling. J. Pers. Med 13 (4). https://doi.org/10.3390/jpm13040649.

D'amelio, M., Cavallucci, V., Cecconi, F., 2010. Neuronal caspase-3 signaling: not only cell death. Cell Death Differ. 17 (7), 1104–1114.

Das R.K., Gogoi N., Babu P.J., Sharma P., Mahanta C., Bora U. (2012) The synthesis of gold nanoparticles using Amaranthus spinosus leaf extract and study of their optical properties.

Dixit, S., Mehra, R.D., Dhar, P., 2020. Effect of α-lipoic acid on spatial memory and structural integrity of developing hippocampal neurons in rats subjected to sodium arsenite exposure. Environ. Toxicol. Pharmacol. 75, 103323.
Engin, A.B., Nikitovic, D., Neagu, M., et al., 2017. Mechanistic understanding of nanoparticles' interactions with extracellular matrix: the cell and immune system. Part Fibre Toxicol. 14 (1), 22. https://doi.org/10.1186/s12989-017-0199-z.
Erel, O., 2005. A new automated colorimetric method for measuring total oxidant status. Clin. Biochem. 38 (12), 1103–1111.
Espadas, I., Ortiz, O., García-Sanz, P., et al., 2021. Dopamine D2R is Required for Hippocampal-dependent Memory and Plasticity at the CA3-CA1 Synapse. Cereb. Cortex 31 (4), 2187–2204.
Firdaus, F., Zafeer, M.F., Ahmad, M., Afzal, M., 2018. Anxiolytic and anti-inflammatory role of thymoquinone in arsenic-induced hippocampal toxicity in Wistar rats. Heliyon 4 (6), e00650.
Flora, S.J., Bhatt, K., Mehta, A., 2009. Arsenic moiety in gallium arsenide is responsible for neuronal apoptosis and behavioral alterations in rats. Toxicol. Appl. Pharmacol. 240 (2), 236–244.
Flurkey K, M., Currer, J., Harrison, D.E., 2007. Chapter 20 - Mouse Models in Aging Research. In: Fox, J.G., Davisson, M.T., Quimby, F.W., Barthold, S.W., Newcomer, C. E., Smith, A.L. (Eds.), The Mouse in Biomedical Research, Second Edition. Academic Press, Burlington, pp. 637–672.
Foyzun, T., Mahmud, A.A., Ahammed, M.S., et al., 2022b. Polyphenolics with strong antioxidant activity from acacia nilotica ameliorate some biochemical signs of arsenic-induced neurotoxicity and oxidative stress in mice. Molecules 27 (3). https://doi.org/10.3390/molecules27031037.
Foyzun, T., Mahmud, A.A., Ahammed, M.S., et al., 2022a. Polyphenolics with Strong Antioxidant Activity from Acacia nilotica Ameliorate Some Biochemical Signs of Arsenic-Induced Neurotoxicity and Oxidative Stress in Mice. Molecules 27 (3), 1037.
Goudarzi, M., Amiri, S., Nesari, A., Hosseinzadeh, A., Mansouri, E., Mehrzadi, S., 2018. The possible neuroprotective effect of ellagic acid on sodium arsenate-induced neurotoxicity in rats. Life Sci. 198, 38–45. https://doi.org/10.1016/j.lfs.2018.02.022.
Granado, N., Ortiz, O., Suárez, L.M., et al., 2008. D1 but not D5 dopamine receptors are critical for LTP, spatial learning, and LTP-Induced arc and zif268 expression in the hippocampus. Cereb. Cortex 18 (1), 1–12.
He, Z., Zhang, Y., Zhang, H., et al., 2021. NAC antagonizes arsenic-induced neurotoxicity through TMEM179 by inhibiting oxidative stress in Oli-neu cells. Ecotoxicol. Environ. Saf. 223, 112554.
Henrich-Noack, P., Nikitovic, D., Neagu, M., et al., 2019. The blood-brain barrier and beyond: Nano-based neuropharmacology and the role of extracellular matrix. Nanomedicine 17, 359–379. https://doi.org/10.1016/j.nano.2019.01.016.
Hou, K., Zhao, J., Wang, H., et al., 2020. Chiral gold nanoparticles enantioselectively rescue memory deficits in a mouse model of Alzheimer's disease. Nat. Commun. 11 (1), 1–11.
Htway, S.-M., Suzuki, T., Kyaw, S., Nohara, K., Win-Shwe, T.-T., 2021. Effects of maternal exposure to arsenic on social behavior and related gene expression in F2 male mice. Environ. Health Prev. Med. 26 (1), 1–10.
Hughes, M.F., Beck, B.D., Chen, Y., Lewis, A.S., Thomas, D.J., 2011. Arsenic exposure and toxicology: a historical perspective. Toxicol. Sci. 123 (2), 305–332.
Ibrahim, E.A., Yousef, M.I., Ghareeb, D.A., et al., 2022. Artichoke leaf extract-mediated neuroprotection against effects of aflatoxin in male rats. BioMed. Res. Int. 2022.
Ishaq S., Siyar S., Basri R., Liaqat A., Hameed A., Ahmed T. (2022) Neuroprotective effects of Shogaol in metals (Al, As and Pb) and high fat diet induced neuroinflammation and behavior in mice. Current Molecular Pharmacology.
Jing, H., Yan, N., Fan, R., et al., 2022. Arsenic Activates the NLRP3 Inflammasome and Disturbs the Th1/Th2/Th17/Treg Balance in the Hippocampus in Mice. Biol. Trace Elem. Res. 1–9.
Karaulov, A.V., Smolyagin, A.I., Mikhailova, I.V., et al., 2022. Assessment of the combined effects of chromium and benzene on the rat neuroendocrine and immune systems. Environ. Res 207, 112096. https://doi.org/10.1016/j.envres.2021.112096.
Katircioğlu, Z., Şakalak, H., Ulaşan, M., Gören, A.C., Yavuz, M.S., 2014. Facile synthesis of "green" gold nanocrystals using cynarin in an aqueous solution. Appl. Surf. Sci. 318, 191–198.
Kim, M., Seo, S., Sung, K., Kim, K., 2014. Arsenic exposure in drinking water alters the dopamine system in the brains of C57BL/6 mice. Biol. Trace Elem. Res. 162 (1), 175–180.
Kumar, M.R., Flora, S., Reddy, G., 2013. Monoisoamyl 2, 3-dimercaptosuccinic acid attenuates arsenic induced toxicity: behavioral and neurochemical approach. Environ. Toxicol. Pharmacol. 36 (1), 231–242.
Kumar, V., Yadav, S.K., 2009. Plant-mediated synthesis of silver and gold nanoparticles and their applications. J. Chem. Technol. Biotechnol.: Int. Res. Process, Environ. Clean. Technol. 84 (2), 151–157.
Kuskov, A., Nikitovic, D., Berdiaki, A., Shtilman, M., Tsatsakis, A., 2022. Amphiphilic Poly-N-vinylpyrrolidone Nanoparticles as Carriers for Nonsteroidal, Anti-Inflammatory Drugs: Pharmacokinetic, Anti-Inflammatory, and Ulcerogenic Activity Study. Pharmaceutics 14 (5). https://doi.org/10.3390/pharmaceutics14050925.
Lin, N., Xiong, L.-L., Zhang, R.-p, et al., 2016. Injection of Aβ1-40 into hippocampus induced cognitive lesion associated with neuronal apoptosis and multiple gene expressions in the tree shrew. Apoptosis 21 (5), 621–640.
Ling, L., Jiang, Y., Liu, Y., et al., 2019. Role of gold nanoparticle from Cinnamomum verum against 1-methyl-4-phenyl-1, 2, 3, 6-tetrahydropyridine (MPTP) induced mice model. J. Photochem. Photobiol. B: Biol. 201, 111657.
Medda, N., Patra, R., Ghosh, T.K., Maiti, S., 2020. Neurotoxic mechanism of arsenic: synergistic effect of mitochondrial instability, oxidative stress, and hormonal-neurotransmitter impairment. Biol. Trace Elem. Res. 198 (1), 8–15.
Mehta, K., Pandey, K.K., Kaur, B., Dhar, P., Kaler, S., 2021. Resveratrol attenuates arsenic-induced cognitive deficits via modulation of Estrogen-NMDAR-BDNF signalling pathway in female mouse hippocampus. Psychopharmacology 238 (9), 2485–2502.
Mioc, M., Pavel, I.Z., Ghiulai, R., et al., 2018. The Cytotoxic Effects of Betulin-Conjugated Gold Nanoparticles as Stable Formulations in Normal and Melanoma Cells. Front Pharm. 9, 429. https://doi.org/10.3389/fphar.2018.00429.
O'Callaghan, C., Shine, J.M., Hodges, J.R., Andrews-Hanna, J.R., Irish, M., 2019. Hippocampal atrophy and intrinsic brain network dysfunction relate to alterations in mind wandering in neurodegeneration. Proc. Natl. Acad. Sci. 116 (8), 3316–3321.
Pandey, R., Rai, V., Mishra, J., Mandrah, K., Kumar Roy, S., Bandyopadhyay, S., 2017. From the cover: arsenic induces hippocampal neuronal apoptosis and cognitive impairments via an up-regulated BMP2/Smad-dependent reduced BDNF/TrkB signaling in rats. Toxicol. Sci. 159 (1), 137–158.
Pandey, R., Garg, A., Gupta, K., et al., 2022. Arsenic Induces Differential Neurotoxicity in Male, Female, and E2-Deficient Females: Comparative Effects on Hippocampal Neurons and Cognition in Adult Rats. Mol. Neurobiol. 59 (5), 2729–2744.
Park, S.Y., Yi, E.H., Kim, Y., Park, G., 2019b. Anti-neuroinflammatory effects of Ephedra sinica Stapf extract-capped gold nanoparticles in microglia. Int. J. Nanomed. 14, 2861.
Park, S.Y., Kim, Y.J., Park, G., Kim, H.-H., 2019a. Neuroprotective effect of Dictyopteris divaricata extract-capped gold nanoparticles against oxygen and glucose deprivation/reoxygenation. Colloids Surf. B: Biointerfaces 179, 421–428.
Prieto, G.A., Tong, L., Smith, E.D., Cotman, C.W., 2019. TNFα and IL-1β but not IL-18 suppresses hippocampal long-term potentiation directly at the synapse. Neurochem. Res. 44 (1), 49–60.
Raghupathi, R., Strauss, K.I., Zhang, C., Krajewski, S., Reed, J.C., McIntosh, T.K., 2003. Temporal alterations in cellular Bax: Bcl-2 ratio following traumatic brain injury in the rat. J. Neurotrauma 20 (5), 421–435.
Ribarič, S., 2021. Nanotechnology Therapy for Alzheimer′ s Disease Memory Impairment Attenuation. Int. J. Mol. Sci. 22 (3), 1102.
Rodrıguez, V., Carrizales, L., Mendoza, M., Fajardo, O., Giordano, M., 2002. Effects of sodium arsenite exposure on development and behavior in the rat. Neurotoxicol. Teratol. 24 (6), 743–750.
Rodríguez-Barranco, M., Gil, F., Hernández, A.F., et al., 2016. Postnatal arsenic exposure and attention impairment in school children. Cortex 74, 370–382.
Sayapina, N.V., Sergievich, A.A., Kuznetsov, V.L., et al., 2016. Influence of multi-walled carbon nanotubes on the cognitive abilities of Wistar rats. Exp. Ther. Med 12 (3), 1311–1318. https://doi.org/10.3892/etm.2016.3495.
Shaji, E., Santosh, M., Sarath, K., Prakash, P., Deepchand, V., Divya, B., 2021. Arsenic contamination of groundwater: A global synopsis with focus on the Indian Peninsula. Geosci. Front. 12 (3), 101079.
Sharma, A., Kshetrimayum, C., Sadhu, H.G., Kumar, S., 2018. Arsenic-induced oxidative stress, cholinesterase activity in the brain of Swiss albino mice, and its amelioration by antioxidants Vitamin E and Coenzyme Q10. Environ. Sci. Pollut. Res. 25 (24), 23946–23953.
Speranza, L., di Porzio, U., Viggiano, D., de Donato, A., Volpicelli, F., 2021. Dopamine: The neuromodulator of long-term synaptic plasticity, reward and movement control. Cells 10 (4), 735.
Subakanman, S., Murugan, S., Devi, P., 2015. Green synthesis of gold nanoparticles using Hypericum hookerianum and its antiparkinson like effect in haloperidol induced swiss albino mice. Int. J. Biol. Chem. 9 (5), 220–234.
Taheri Zadeh, Z., Esmaeilpour, K., Aminzadeh, A., Heidari, M.R., Joushi, S., 2021. Resveratrol attenuates learning, memory, and social interaction impairments in rats exposed to arsenic. BioMed. Res. Int. 2021.
Takeuchi, T., Duszkiewicz, A.J., Sonneborn, A., et al., 2016. Locus coeruleus and dopaminergic consolidation of everyday memory. Nature 537 (7620), 357–362.
Vucinic, S., Antonijevic, B., Tsatsakis, A.M., et al., 2017. Environmental exposure to organophosphorus nerve agents. Environ. Toxicol. Pharmacol. 56, 163–171.
Wallace, D.R., Taalab, Y.M., Heinze, S., et al., 2020. Toxic-metal-induced alteration in miRNA expression profile as a proposed mechanism for disease development. Cells 9 (4), 901.
Wang, X., Huang, X., Zhou, L., et al., 2021. Association of arsenic exposure and cognitive impairment: A population-based cross-sectional study in China. Neurotoxicology 82, 100–107.
Xiong, L., Huang, J., Gao, Y., et al., 2021. Sodium arsenite induces spatial learning and memory impairment associated with oxidative stress and activates the Nrf2/PPARγ pathway against oxidative injury in mice hippocampus. Toxicol. Res. 10 (2), 277–283.
Xue, J., Liu, T., Liu, Y., et al., 2019. Neuroprotective effect of biosynthesised gold nanoparticles synthesised from root extract of Paeonia moutan against Parkinson disease–In vitro & In vivo model. J. Photochem. Photobiol. B: Biol. 200, 111635.
Zha, Z., Liu, S., Liu, Y., Li, C., Wang, L., 2022. Potential utility of natural products against oxidative stress in animal models of multiple sclerosis. Antioxid. (Basel) 11 (8). https://doi.org/10.3390/antiox11081495.
Zucker, I., Beery, A.K., 2010. Males still dominate animal studies, 690-690 Nature 465 (7299). https://doi.org/10.1038/465690a.